A SEMI-EMPIRICAL MODEL OF THE TENSILE ENERGY ABSORPTION OF SACK KRAFT PAPER

Paul Shallhorn and Norayr Gurnagul *

We have developed a semi-empirical model to relate the tensile energy absorption (TEA) of paper sheets formed from high-consistency refined pulp to pulp properties, including water retention value (WRV), fibre length, and fibre curl. TEA is shown to be related to the normalized stretch (ratio of stretch to tensile strength) and the tensile strength of the pulp. Normalized stretch appears to be a function of fibre curl, whereas tensile strength for a given pulp is a function of the fibre length, fibre curl, and WRV. The manner in which these three pulp properties develop in a given refining operation determines the development of TEA.

Keywords: Kraft papers; Bag papers; Rupture work; Pulp properties; Paper properties; Water retention; Tensile strength; Stretch; Toughness; Fiber length; Mathematical models

*Contact information: FPInnovations-Paprican, 570 Blvd. St-Jean, Pointe-Claire, Quebec, H9R 3J9, Canada 1000, *Corresponding author: norayr.gurnagul@fpinnovations.ca*

INTRODUCTION

Critical properties of paper for sack grades are high tensile energy absorption (TEA) and relatively low air flow resistance. This makes a tough paper resisting impact stress during handling of the sack and a paper that lends itself to easy filling of the sack.

High-consistency refining (HCR) is used to treat softwood kraft fibres to give a paper of high TEA and relatively low air resistance. HCR induces curl and microcompressions in the fibres; these effects enhance sheet stretch significantly while increasing tensile strength and air resistance moderately. Recently, work at FPInnovations-Paprican and elsewhere has shown that pressurized HCR gives a higher TEA at a given level of air resistance compared to conventional atmospheric HCR (Sjöberg and Höglund 2005; Gurnagul et al. 2009).

There appears to be no model in the literature on the role of fibre properties in the development of TEA. It is known that curl and microcompressions influence stretch positively and curl influences tensile strength negatively (Page et al. 1985), but no model pulls these observations together to explain how TEA varies with changes in curl, microcompressions, and other fibre properties.

This report attempts to develop a semi-empirical model of TEA as a function of fibre properties for freely dried paper made from softwood kraft pulp refined at high consistency both under atmospheric and pressurized conditions.

EXPERIMENTAL

The pulps used in this study were obtained from two mills manufacturing sack kraft paper, one using bleached softwood kraft and one using unbleached softwood kraft. The pulps were sampled at the exit of the twin-roll press sections prior to high-consistency refining at each mill. This study applies the TEA model to a number of HCR pulps from the two mills.

A sample of unbleached pulp was subjected to pilot plant high-consistency refining under atmospheric conditions with a Bauer 36-inch atmospheric discharge refiner (plate pattern Bauer 36104). An analysis of the refined pulp in terms of refining intensity was reported earlier (Gurnagul et al. 2006). The unbleached pulp was only refined under atmospheric conditions. Another sample of unbleached pulp from the same mill was subjected to atmospheric (using the same Bauer refiner as described above) and pressurized HCR refining. The pressurized high-consistency refining was done with a 22-inch pressurized Andritz refiner, which includes a screw plug feeder to provide pressurized conditions (Gurnagul et al. 2009). A sample of bleached pulp was refined under both atmospheric and pressurized conditions (Gurnagul et al. 2009). Standard procedures of PAPTAC were followed for the measurement of fibre, pulp, and sheet properties. The fibre length, curl, and kink measurements were made with a HiRes Fibre Quality Analyzer (Optest Equipment, Hawkesbury, Ontario, Canada). More details can be found in Gurnagul et al. (2006). Water retention value, WRV, was measured using Tappi Useful Method UM 256.

RESULTS AND DISCUSSION

Model

Tensile energy absorption is defined as the integral of the tensile force and specimen elongation up to the point of sheet failure and is expressed in units of J/m^2 (work per unit specimen area), or J/g if the former unit is corrected for grammage. If the force-elongation curve of the specimen under tensile testing were linear (i.e. totally elastic behaviour), TEA would be equal to simply one-half of the product of the tensile strength and the stretch, corrected for units of course. However, the tensile-stretch curve of paper is non-linear, being elastic initially but showing non-elastic behaviour as it apparently yields. Despite this non-linearity, El-Hosseiny (1994) found that TEA is still proportional (not equal) to the one-half product of tensile strength and stretch for standard handsheets of various kraft pulps. Also, the same relationship was found true for freely dried handsheets of unbleached softwood kraft pulp, which simulates sack paper (Gurnagul et al. 2006). The proportionality factor was found to be about 1.3 for a number of pulps (the factor would be unity for an elastic strength-stretch curve). This proportionality will be assumed to be true in the model developed. To simplify matters, the model discusses separately the relationship between fibre properties and stretch, and the relationship between fibre properties and tensile strength. Once the relationships for stretch and tensile strength are established, it is a simple matter to combine them to give the product of stretch and tensile strength, which is assumed proportional to TEA.

Stretch

Seth has shown that sheet extensibility depends primarily on two factors – the stretch-potential of fibres and the degree of bonding between them; better bonding allows greater use of the stretch-potential (Seth 2005a). The fibre's stretch potential is controlled by the extent of misalignment of the cellulose fibrils in the fibre wall with respect to the fibre axis. The misalignment may be inherent, as in the case of fibres with high fibril angle, or induced by axial compression of the fibre wall as is the case during high-consistency refining.

In high-consistency refining, the stretch potential of fibres is controlled by the extent of induced microcompressions (Seth 2005a). The stretch of paper under a given tensile stress (or level of bonding) is thus assumed to be proportional to the number and elongation of the microcompressions in an average fibre. An indirect corroboration of the assumption is found in the work of Kibblewhite (1976) who found that in high-consistency lab refining, the stretch of paper at a given tensile was proportional to the number of fibre wall fractures, which are related to changes in internal fibre structure with high-consistency beating. Unfortunately, there is currently no quantitative method to measure the number and character of microcompressions.

In this work, an indirect measure of microcompressions is applied which utilizes the assumption that the number of microcompressions per fibre is proportional to the number of kinks per fibre. This assumes that some of the microcompressions, presumably the largest, are points on the fibre where significant changes in fibre axis direction (i.e., kinks) occur. The general supposition is that the greater the number of kinks, the more the number of microcompressions.

From the Fibre Quality Analyzer (FQA) (Optest HiRes model) data for a typical HCR softwood pulp, the average number of significant kinks (kinks with kink angle greater than 20 degrees, the minimum angle that the FQA records per fibre) is of the order of zero to five for individual fibres. Being a measurement in terms of integers of small value, it is believed that this measure is not very precise. Instead, the related measurement of curl, being a distance measurement of the actual fibre length, L, divided by the fibre end-to-end distance, L_{ee}, is more precise, and is therefore preferable.

The assumption is made that measured fibre kinks are related to fibre curl, where abrupt changes in fibre direction cause the fibre curliness. This is mentioned by Seth (2005b) and is apparent in photomicrographs of so-called curly fibres in his paper. Fibre curl of circular arcs is rare, especially in HCR pulps, so this type of curl is not considered in this discussion. To test the assumption that fibre curl is derived from the number of fibre kinks, theory from polymer physics is used (De Gennes 1979). A curled fibre can be conceived as a two-dimensional entity made up of a number of straight segments of random direction and random length separated by kinks. This is analogous to a two-dimensional polymer made up of a string of monomers oriented in different directions. Polymer physics states that the mean square root distance of the end-to-end distance, L_{ee}, of the polymer is related to the number of monomers, N, by the relation, $L_{ee} = aN^{\nu}$, where a is some average length of the monomer, and the exponent ν depends on the dimensionality of the polymer. For two-dimensional self-avoiding polymers, theory and simulations indicate that $\nu = ¾$ (De Gennes 1979).

The curl index C for a fibre, as measured by the Optest FQA, is defined as $C = L/L_{ee}$ -1. For a fibre, $L=Na$, and if we assume $L_{ee} = aN^{3/4}$, where N and a are the average number and length of segments between kinks in a fibre, respectively. Thus,

$$C+1 = N^{1/4} \quad (1)$$

and K, the number of kinks per fibre, is simply given by $K = N$-1. The FQA measures k, the number of kinks per mm, and L_a, the arithmetic fibre length, so that K, the number of kinks per fibre, is given by $K = kL_a = N$-1. Because we are linking the number of kinks per fibre to the curl of a fibre, C_a, the arithmetic fibre curl, is the most appropriate FQA curl index to use in this case. Therefore,

$$C_a+1 = (K+1)^{1/4} = (kL_a+1)^{1/4} \quad (2)$$

Thus, this hypothesis that arithmetic curl, C_a, is related to the K, the number of kinks per fibre, by equation 2 can be tested by a plot of $\ln(C_a+1)$ versus $\ln(kL_a+1)$. Figure 1 for HCR unbleached kraft pulp refined under atmospheric conditions gives the regression equation $C_a+1= 0.95(kL_a+1)^{0.25}$ (the standard error of the exponent 0.25 being 0.02). Figure 2 for HCR unbleached pulp under both atmospheric and pressurized refining conditions yields a regression equation of $C_a+1= 0.98(kL_a+1)^{0.27}$ (the standard error of the exponent 0.27 being 0.04). Figure 3 for a different sample of HCR bleached kraft pulp refined under atmospheric and pressurized conditions yields $C_a+1= 0.99 (kL_a+1)^{0.26}$ (the standard error of the exponent 0.26 being 0.10).

In Figs. 2 and 3, there is considerable scatter, which is due primarily to the pressurized data in these graphs. Except for the fact the pressurized data contain high values of curl and kink, the reason for this is not known. Despite the scatter, the regression equation expressions for these different pulps are remarkably close to the expression given by equation 2. This tends to validate the assumed relation between FQA curl and kink measurements. This means that K, the number of kinks per fibre, can be calculated from arithmetic curl as $(C_a+1)^4$-1, using equation 2. This is felt to be a more precise measurement of K rather than kL_a, which incorporates the imprecise measurement of k. Kink measurements on a fibre are restricted to whole numbers, whereas curl can be measured as the ratio of two length measurements to a precision set by the pixel resolution of the FQA.

Now, the average number of microcompressions per fibre is assumed proportional to K, the average number of kinks per fibre, so that in terms of curl measurement, n_m, the number of microcompressions per fibre, is then proportional to $(C_a+1)^4$-1, i.e.,

$$n_m = \alpha K = \alpha[(C_a+1)^4 - 1)] \quad (3)$$

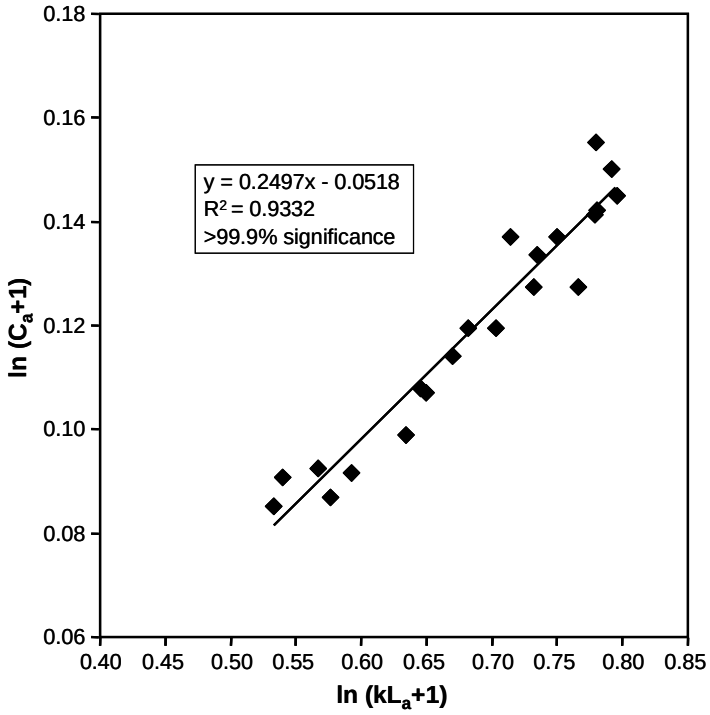

Fig.1. Verification of equation 2 for **unbleached kraft** pulp refined in an atmospheric high-consistency refiner

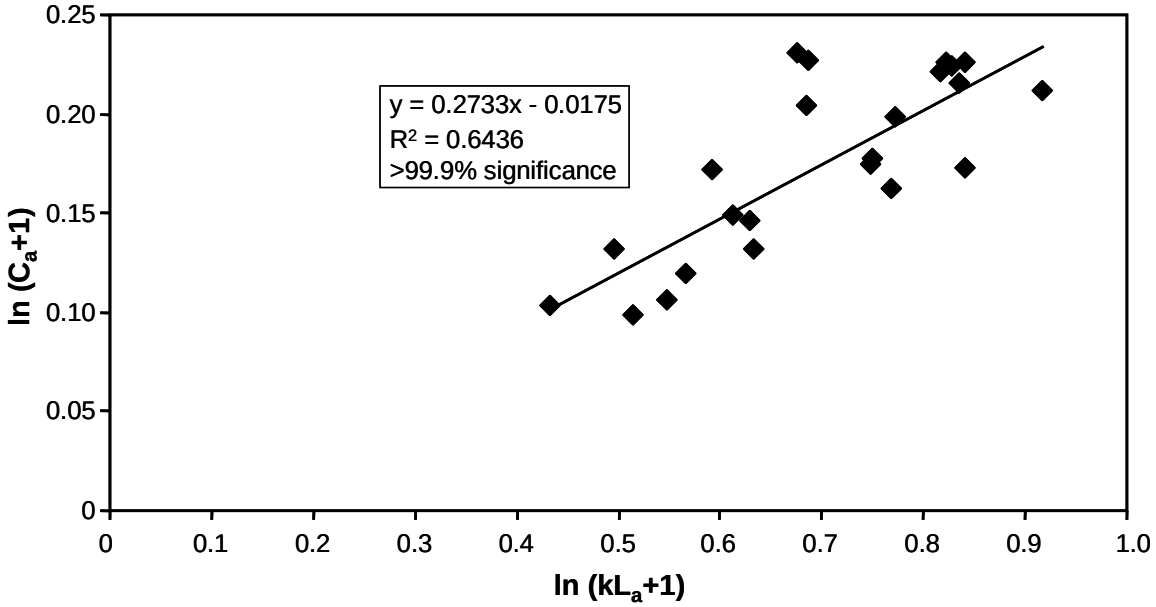

Fig. 2. Verification of equation 2 for **unbleached kraft** pulp high-consistency refined under atmospheric and pressurized conditions

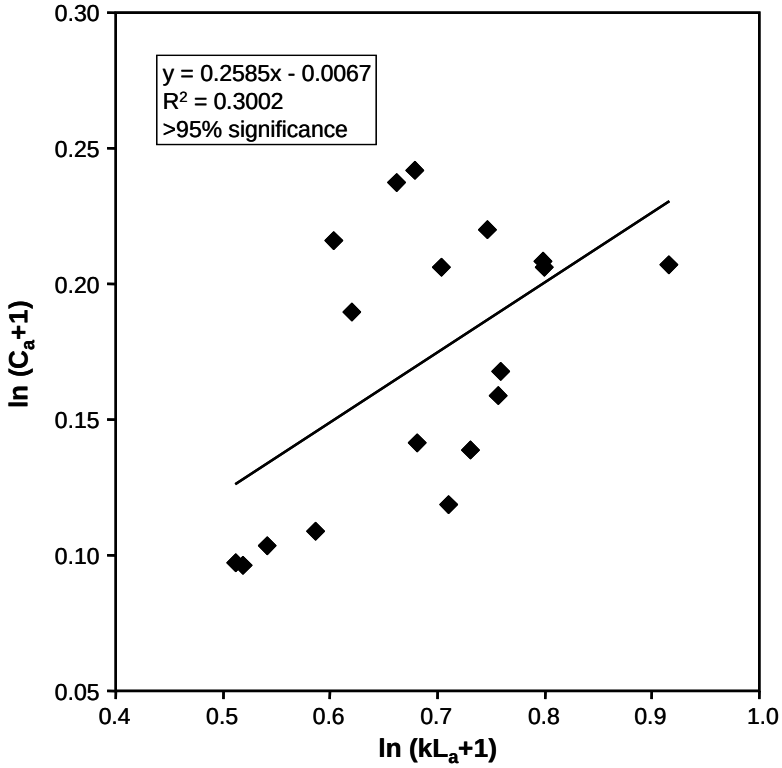

Fig.3. Verification of equation 2 for **bleached kraft** pulp high-consistency refined under atmospheric and pressurized conditions

It is assumed that the stretch-to-break of a freely-dried sheet, normalized by dividing by tensile strength, is a measure of its ultimate extensional behaviour and that this is related to n_m and hence, the average number of kinks per fibre or fibre curl through equation 3. Henceforth, this stretch to break measure will be referred to as the normalized stretch.

This assumption is tested in Fig. 4 for data on unbleached atmospheric and pressurized HCR softwood kraft pulp. A good linear correlation is found with intercept 0.03 (standard error of 0.01), which is the assumed normalized stretch for a kink-free fibre. A never-dried laboratory unbleached black spruce kraft beaten in a PFI mill to 12000 revolutions to remove most of the curl has roughly a stretch and tensile index of 3.9 % and 141 N·m/g respectively (Seth 1990) giving a normalized stretch value of 0.03 in general agreement with the intercept value in Fig. 4. For bleached atmospheric and pressurized refined pulp, Fig. 5 also indicates a good linear relation between normalized stretch and $[(C_a+1)^4-1]$ with a similar intercept of 0.04 in this case. The slope of the figures is the stretch potential per unit kink or, in engineering terms, the compliance of the fibre per kink.

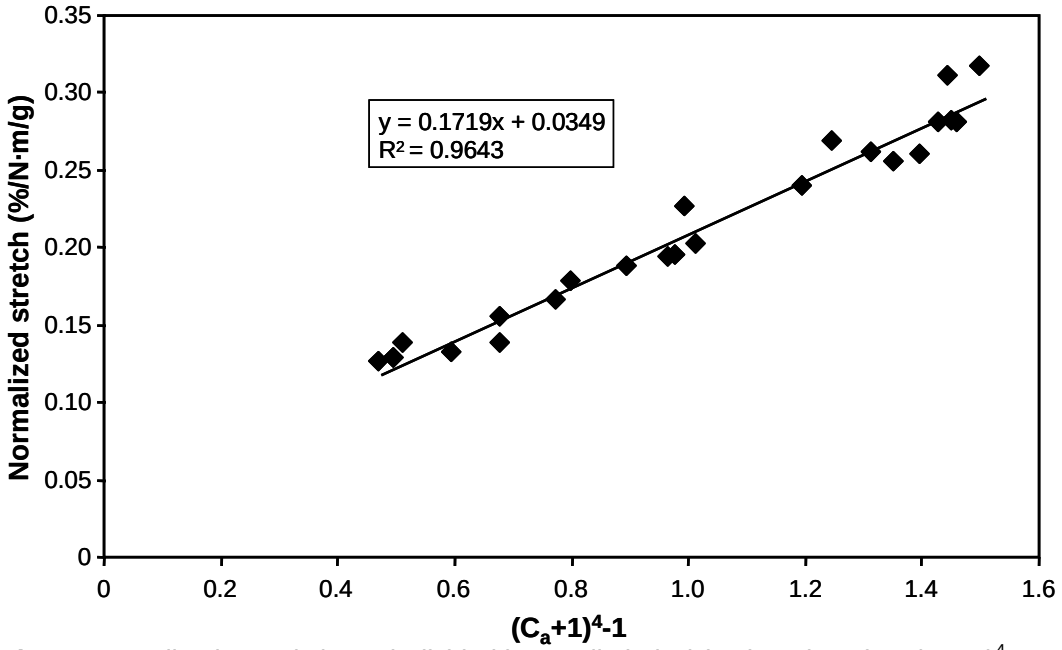

Fig. 4. Normalized stretch (stretch divided by tensile index) is plotted against $(C_a+1)^4-1$, where C_a is the arithmetic curl index. This expression is assumed to be proportional to the number of microcompressions per fibre as explained in equation 3. The data are for **unbleached kraft** pulp refined under atmospheric and pressurized conditions.

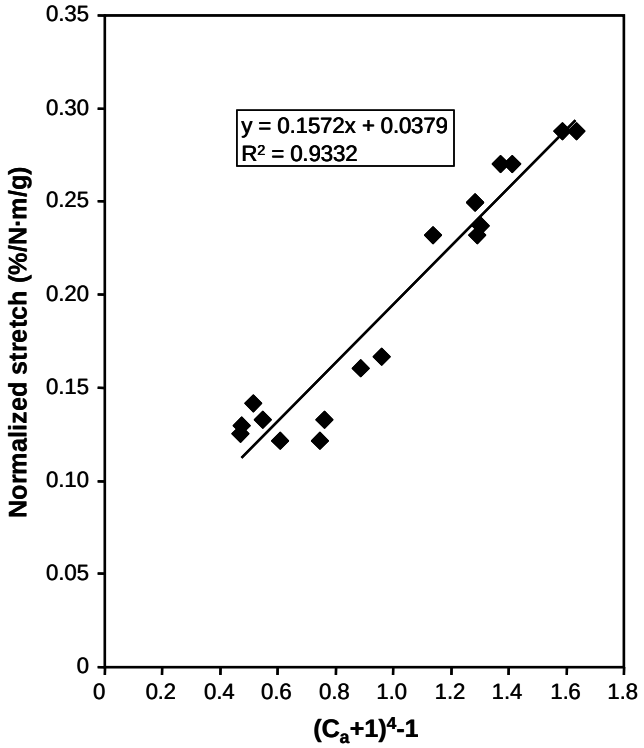

Fig. 5. Normalized stretch is plotted against $(C_a+1)^4-1$ for **bleached kraft** pulp refined under atmospheric and pressurized conditions.

Tensile strength

Page's equation (Page 1969) for the tensile strength, T, in units of N·m/g, of a paper made up of straight fibres can be expressed as:

$$\frac{1}{T} = \frac{9}{8Z} + \frac{12C_s}{PLbRBA} \quad (4)$$

where Z is the zero-span tensile strength (strength for a well bonded paper, also considered to be an index of fibre strength), C_s is fibre coarseness, P is fibre perimeter, L is the fibre length assuming straight fibres, b is the shear strength of fibre-to-fibre bonds, and RBA is relative bonded area. This equation must be adapted to freely dried paper made of curled and microcompressed fibres. The factors C_s, P, and b are not expected to change significantly with curled fibres but Z and L are expected to change. Changes in b with refining have been noted but are much less important than changes in fibre conformability or RBA (Mohlin 1975). Seth has found that curl reduces zero span strength considerably (Seth 2001). However, because Z is usually much greater than T, variations in Z due to fibre curl do not change T appreciably for small RBA due to the form of equation 4. For example, using typical values of Z and T from atmospheric and pressurized HCR bleached pulp in this study, for a constant second term in the right side of equation 4, if Z decreases by 20% from a presumed initial value of 150 to a value of 120 N.m/g, T decreases from a presumed initial value of 50 to a value of 46 N.m/g, only an 8% decrease.

It has been shown by Paavilainen that RBA correlates linearly with pulp water retention value (WRV) (Paavilainen 1990). This means that RBA, an important factor in paper tensile strength, can be linked to a pulp property, WRV. This is advantageous for the prediction of paper strength from pulp properties. Figure 6 is a plot of RBA(%) against WRV using data from Table 3 in (Paavilainen 1990). It is plausible that a higher WRV lowers the cell wall wet elastic modulus, resulting in enhanced collapsibility and/or conformability of fibres, which in turn gives rise to a higher RBA under a given wet pressing pressure. The slope of the linear relation decreases for summerwood fibres (Fig. 6). Data of Paavilainen indicate that the slope of the plots between RBA and WRV decrease with increasing coarseness; a coarser softwood pulp has a greater cell wall thickness, which would give rise to a lower RBA for a given WRV and wet pressing pressure (Paavilainen 1993). The plot also shows that RBA becomes zero at some finite value of WRV; this could be related to fibre properties and WRV measurement used on the pulp. From Paavilainen's work, we assume for a given pulp:

$$RBA = \beta(WRV - WRV_0) \quad (5)$$

where β is a proportionality constant that is influenced, among other things, by coarseness in an inverse fashion, and WRV_0 is the extrapolated value of WRV for zero RBA or zero tensile strength.

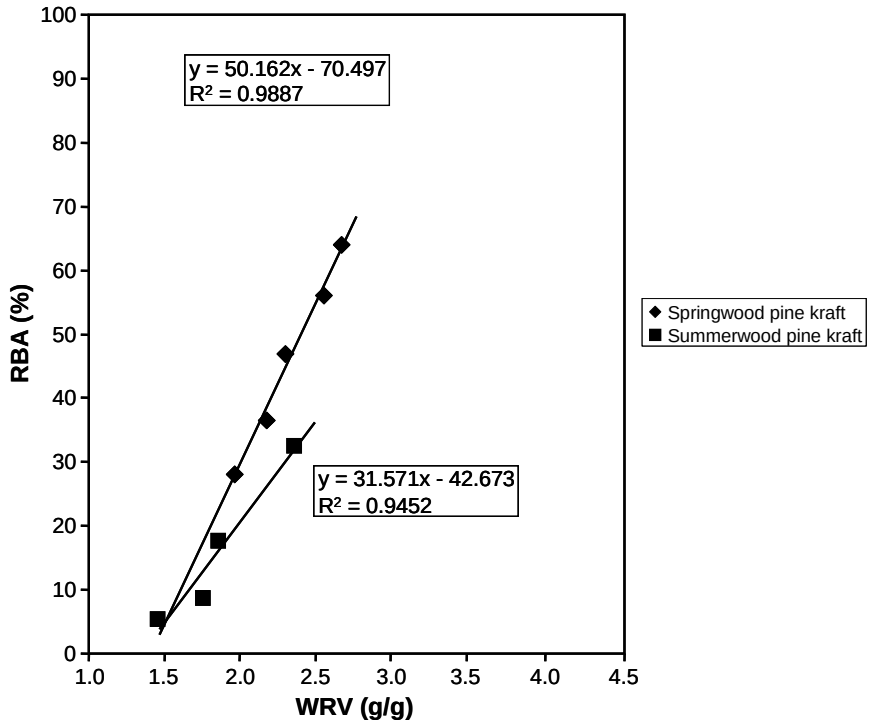

Fig. 6. Relative bonded area (RBA) is plotted against water retention value (WRV) for springwood and summerwood pine kraft pulps (Paavilainen 1990).

For small *RBA*, equation 4 predicts that *T*, the tensile strength of paper, is proportional to *RBA* for a given pulp (assuming fibre dimensions and shear bond strength remain relatively constant as *RBA* varies). Thus, assuming equation 5, a plot of *T* versus *WRV* should give a linear relation for small tensile values (low levels of bonding). This is seen in Figs. 7 and 8 for the pulps in this study; the flattening off of the curve at high *WRV* is attributed to the limiting value of (8/9)*Z* according to Page's equation, *Z* being the zero-span tensile strength, for tensile strength at large values of *RBA*. For these pulps, WRV_0 is 0.8 g/g in Fig. 7 and 0.6 g/g in Fig. 8 in contrast to 1.4 g/g for both pulps in Fig. 6.

A graph in a paper by Mohlin also gives a linear relation between *T* and *WRV* at low tensile values for a bleached softwood kraft beaten in different refiners (Mohlin 1992). The value of WRV_0 in this case is about 0.8 g/g. The differing values of WRV_0 are attributed possibly to different fibre properties and somewhat different measurement techniques. The key point is *RBA* increases with increasing *WRV* according to equation 5, where β and WRV_0 depend on the pulp and measurement. Assuming that *RBA* is linearly related to the light scattering coefficient, equation 5 predicts that scattering coefficient is linearly related to *WRV*, a prediction supported by Mohlin (1992).

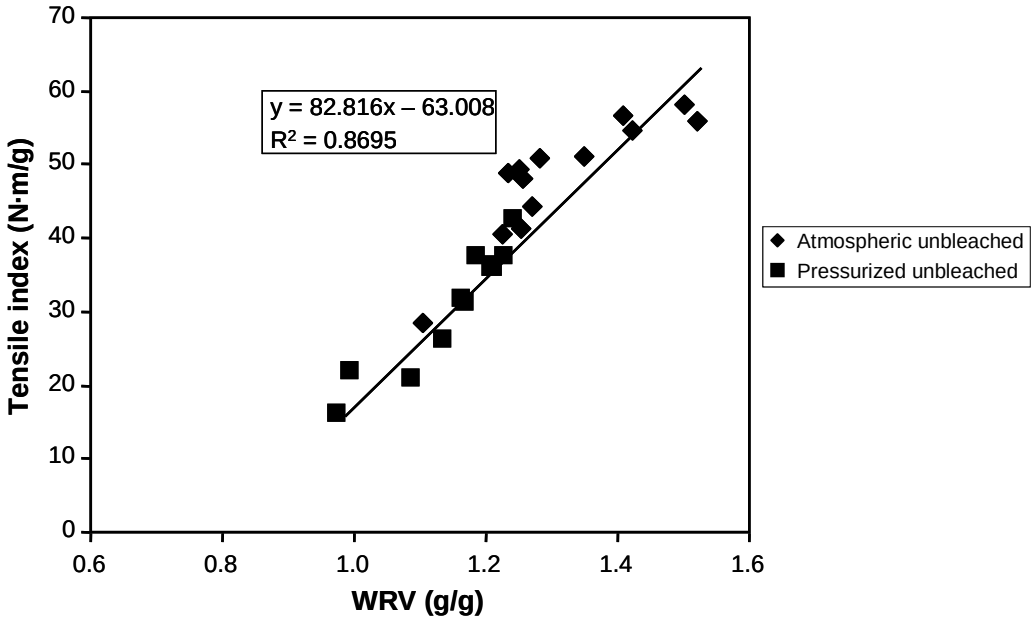

Fig. 7. Tensile strength is linearly correlated with *WRV* assuming that shear bond strength remains relatively constant with refining. The data are for **unbleached kraft** pulp refined under atmospheric and pressurized conditions.

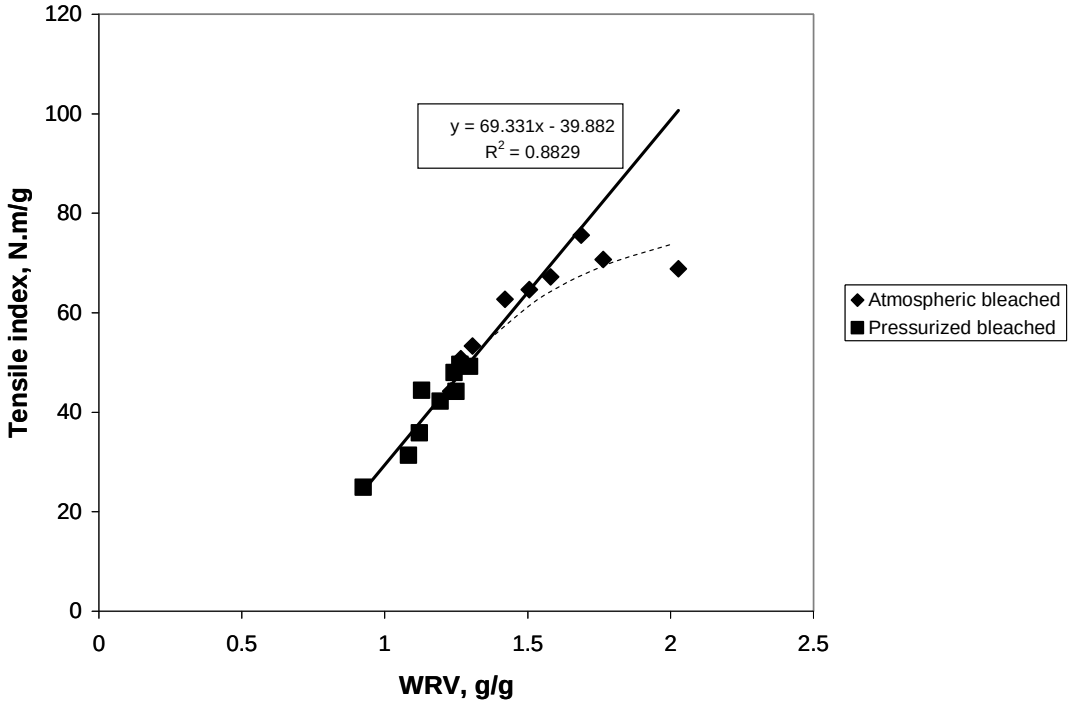

Fig. 8. A plot of tensile strength against *WRV* for **bleached kraft** pulp refined under atmospheric and pressurized conditions is also linear. The flattening off of the curve at high *WRV* is attributed to the limiting value of *(8/9)Z* according to the Page equation where *Z* is the zero-span tensile strength.

Page's equation assumes that all fibres that take up load in tensile testing are straight. However, for an assembly of fibres of different curl, this is not true, because for a given fibre orientation to the load, straight fibres take up more load than curly fibres. This means that the paper breaks at a lower load, because only a fraction of the fibres support the load. A means to incorporate this effect is to assume a shorter effective fibre length. Page *et al.* qualitatively account for lower tensile with curled or kinked fibres as due to a shorter effective fibre length (Page et al. 1985). An assumption is made that the effective fibre length is the end-to-end length of the fibre, L_{eff}, so that

$$L_{eff} = \frac{L_w}{(C_w + 1)} \tag{6}$$

where L_w and C_w is the length-weighted fibre length and curl respectively. L_w and C_w are used here because the derivation of Page's equation assumes the long fibre fraction bears the tensile stress. In effect, L_{eff} is the uniform length of an assembly of straight fibres assumed to give rise to the same tensile strength as the actual fibres of length L_w and uniform curl C_w. Substituting equations 6 and 5 in equation 4, one has:

$$\frac{1}{T} = \frac{9}{8Z} + \frac{\gamma(C_w + 1)}{L_w(WRV - WRV_0)} \tag{7}$$

where $\gamma = \frac{12C_s}{P\beta b}$.

There is some justification for this particular adjustment of fibre length in Page's equation for curled fibres. The Appendix gives a derivation of equation 6 with simplifying assumptions. In addition, Patel and Kothari find the tensile load for non-woven fabrics to be inversely proportional to (C+1) for hookean (purely elastic) fibres, where C is the curl index for all fibres (Patel and Kothari 2001).

Since fibre coarseness or perimeter values were not measured in this study, an approximate value of γ is calculated as follows. Using typical unbleached softwood kraft pulp fibre values, C_s ~160 × 10^{-6} g/m, P ~ 80 × 10^{-6} m, β is the average slope of the two lines in Fig. 6 when RBA is in fractional units (not percentage as Fig. 6) or approximately 0.4, b ~ 6 × 10^6 N/m^2 (Seth 1990), and if L_w is in units of mm, γ ~ 0.010.

Figures 9 and 10 are plots of equation 7 using the data for the unbleached and bleached pulps refined under both atmospheric and pressurized conditions in this study. The satisfactory fit obtained justifies the assumptions made to modify Page's equation for curly fibres. The slope of 0.017 in Figs. 9 and 10 is larger than the value 0.010 calculated above but considering the approximate nature of the calculation, the agreement is satisfactory, being in the same order of magnitude. The intercepts of Figs. 9 and 10 give a value of Z of 256 and 152 N·m/g, respectively. No zero span tensile tests were done on these pulps. However, zero span tests on a more recent sample of bleached pulp from the same source gave Z = 120 to 150 N·m/g for the pressurized and atmospheric refined samples, respectively. The value of 256 N·m/g for the unbleached pulp appears high; this is likely related to the high coefficient of variation (48%) in the intercept of Fig. 9.

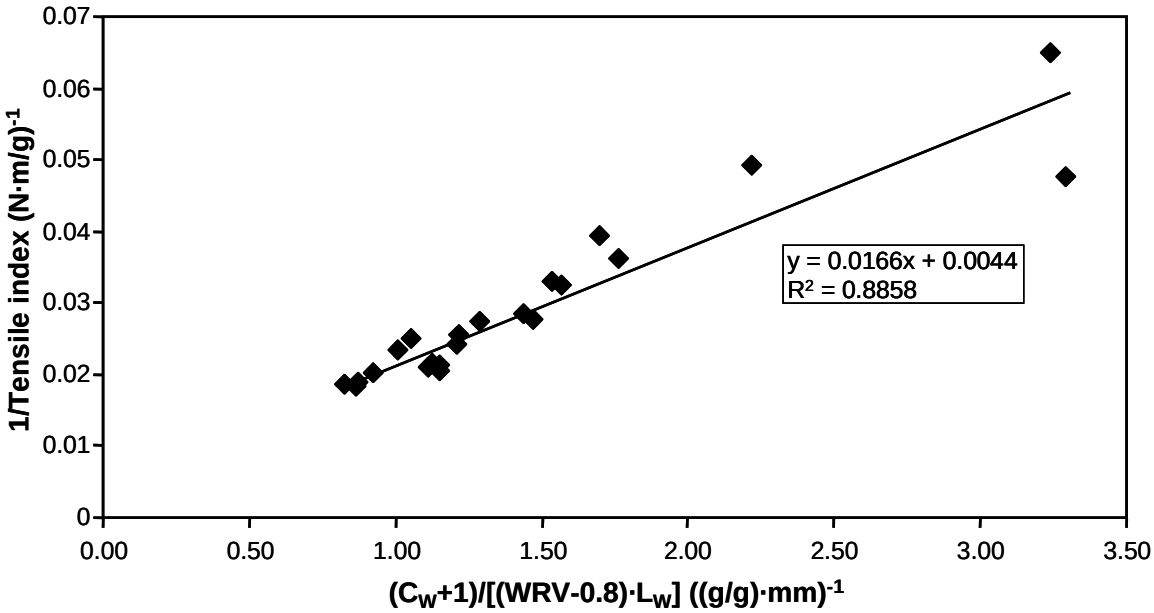

Fig. 9. A plot of equation 7 is shown relating tensile strength to length-weighted curl index C_w, length-weighted average fibre length, L_w, and *WRV* for **unbleached kraft** pulp refined under atmospheric and pressurized conditions.

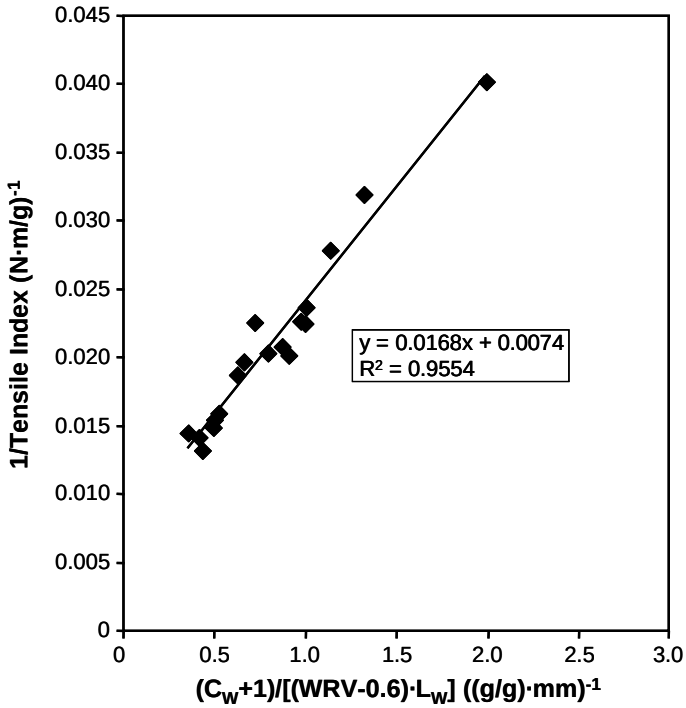

Fig. 10. A plot of equation 7 using data for **bleached kraft** pulp refined under atmospheric and pressurized conditions

Tensile Energy Absorption (TEA)

Gurnagul et al. (2006) have shown for the unbleached pulp refined under atmospheric conditions only that the *TEA* index correlates extremely well with the product of tensile index and stretch (expressed as a ratio of elongation per unit length, not as a percentage). This is also true for the bleached pulps, as shown in Fig. 11, where *TEA* is plotted against one-half the product of tensile index and stretch.

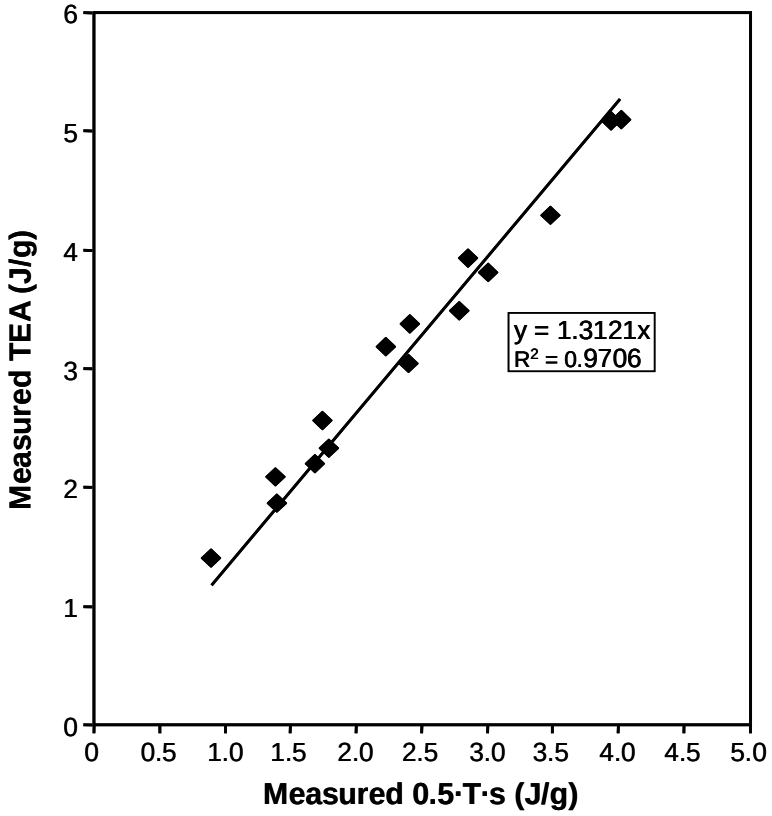

Fig. 11. The measured *TEA* index is plotted against the product of tensile index and stretch or elongation (elongation is expressed as a ratio, not as a percentage). The data are for **unbleached kraft** pulp refined under atmospheric and pressurized conditions.

If the tensile-stretch curve was linear, the slope of the regression equation would be unity; however, the curve is usually non-linear and slopes of roughly 1.3 are obtained. The slopes in the two cases, unbleached and bleached pulps, are 1.29 (Gurnagul et al. 2006) and 1.31, respectively, which are quite close, considering experimental error in the data. This analysis of TEA in terms of tensile strength and stretch can be expressed as:

$$TEA = \eta(0.5Ts) = \eta(0.5)(\frac{s}{T})(T^2) = \eta(0.5)\ \frac{\left(\frac{s}{T}\right)}{\left(\frac{1}{T}\right)^2} \qquad (8)$$

where T is the tensile index, s is the stretch as a ratio, and η is the proportionality constant, which is about 1.3, as discussed above. The last two equalities in equation 8 indicate that normalized stretch s/T and $1/T$ can be used rather than s and T to calculate TEA. Now, the regression equation in Fig. 4 gives the normalized stretch as a function of curl as explained previously, and the regression equation in Fig. 9 gives $1/T$ as a function of fibre length, curl, and WRV. The TEA was calculated for the unbleached pulp subjected to both atmospheric and pressurized refining using equation 8 and the regression equations for s/T and $1/T$ from Figs. 4 and 9 respectively, as follows:

$$\frac{s}{T} = 0.00035 + 0.00172[(C_a + 1)^4 - 1] = -0.00137 + 0.00172\left(C_a + 1\right)^4 \quad (9)$$

$$\frac{1}{T} = 0.0044 + 0.0166\frac{C_w + 1}{L_w(WRV - 0.8)} \quad (10)$$

Note that s in equation 9 above is expressed as a ratio, not in units of percentage as in the normalized stretch in the regression equation of Fig. 4. The correlation in Fig. 12 is very good, and the slope of 1.5 is close to the value 1.3 found by Gurnagul et al. (2006).

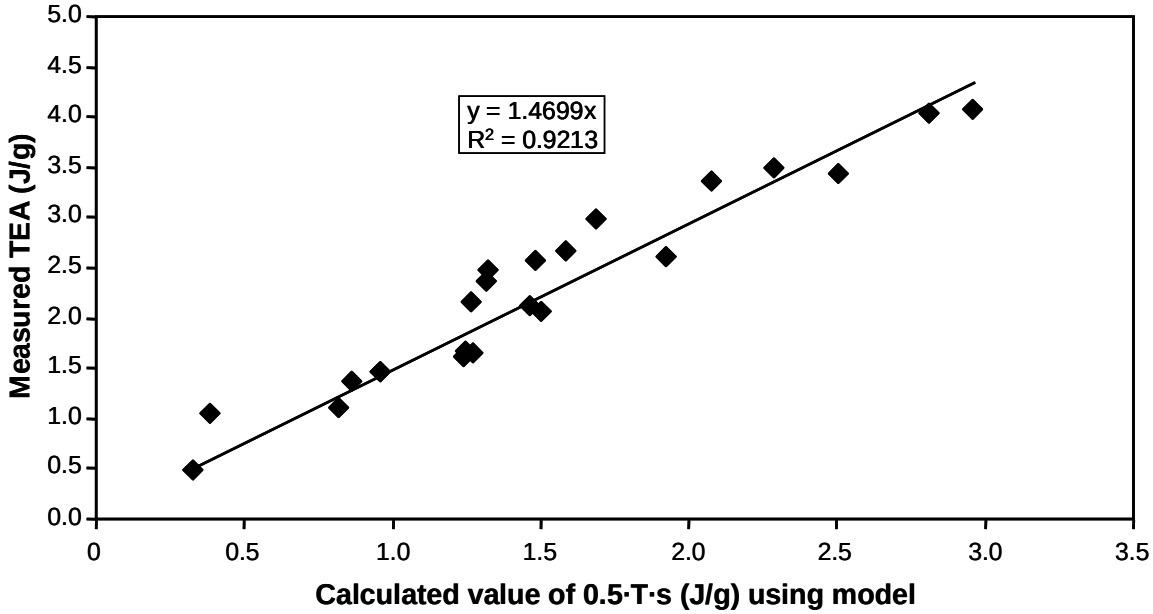

Fig. 12. This plot shows the measured *TEA* index against a calculated *TEA* index using our model. The *TEA* index was calculated using equation 8 and the regression equations for *s/T* and *1/T* from Figures 4 and 9 respectively (see equations 9 and 10). The data are for **unbleached kraft** pulp refined under atmospheric and pressurized conditions.

For the bleached pulp, equation 8 is shown in Fig. 13, using the regression equations for s/T and $1/T$ from Figs. 5 and 11, respectively, as follows:

$$\frac{s}{T} = 0.00038 + 0.00157[(C_a + 1)^4 - 1] = -0.00119 + 0.00157\left(C_a + 1\right)^4 \quad (11)$$

$$\frac{1}{T} = 0.0074 + 0.0168\frac{C_w + 1}{L_w(WRV - 0.6)} \quad (12)$$

Again, note that *s* in equation 11 above is expressed in units of a ratio, not in units of percentage as in the normalized stretch in the regression equation of Fig. 5. The correlation in Fig. 13 of the measured value of *TEA* for the bleached HCR pulps with the value of *TEA* calculated from equations 8, 11, and 12 is good, and the slope η of 1.2 is close to the value 1.3 found in Fig. 11. The rightmost point in Fig. 13 appears significantly off the regression line for unknown reasons. However, this point represents the highest energy run of Table 1 of 715 kW·h/t, which is quite outside the commercial range of about 300 kW·h/t, and therefore, is not commercially relevant.

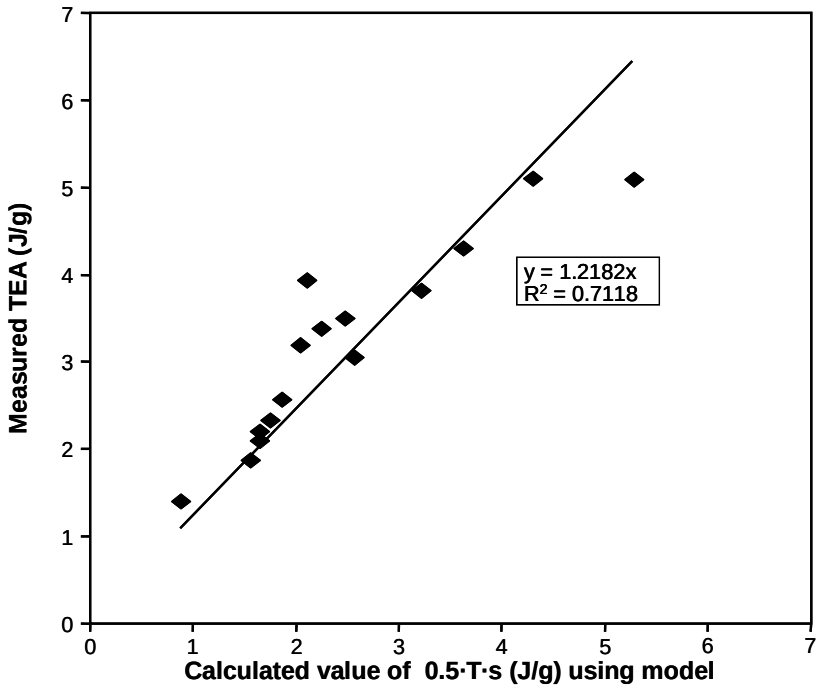

Fig. 13. The measured *TEA* index is plotted against a calculated *TEA* index using our model. The data are for **bleached kraft pulp** refined under atmospheric and pressurized conditions. The *TEA* index was calculated using equation 8 and the regression equations for *s*/*T* and 1/*T* from Figs. 5 and 10 respectively (see equations 11 and 12).

Summary of the TEA Model

The model to determine the TEA of a pulp from its wet and dry properties has been developed in the preceding discussions. It is necessary at this stage to recapitulate the formulation of this semi-empirical model, which uses empirical relations based on theoretical discussion.

Firstly, *s/T* is plotted against $(C_a+1)^4$-1 and a linear regression equation is extracted (see Fig. 4 for example), of the form:

$$\frac{s}{T} = a_0 + a_1[(C_a+1)^4 - 1] \quad (13)$$

where a_0 = 0.00035 and 0.00038, and a_1 = 0.0017 and 0.0016, for unbleached and bleached kraft (both atmospheric and pressurized), respectively. The closeness of the values of a_0 and a_1 for both pulps indicates that this equation with the average values of a_0 and a_1 above, 0.00037 and 0.0016 respectively, substituted in the equation is applicable to all HCR pulps at least in our laboratory. The physical interpretation of a_0 is the stretch potential of straight-fibred pulp with no curl or kinks, and a_1 is the change in stretch potential per fibre kink. Further work is required to derive these coefficients from more basic fibre properties.

1/T is plotted against $(C_w+1)/[L_w(WRV-WRV_0)]$ (see Fig. 9 for example where WRV_0 = 0.8 in this study) and a linear regression extracted of the form:

$$\frac{1}{T} = b_0 + b_1 \frac{C_w + 1}{L_w(WRV - WRV_0)} \quad (14)$$

where WRV_0 is found from a plot of *T* against *WRV* for small values of *T* where linearity is observed (see Fig. 6 for example). The coefficient b_0 equals 0.004 and 0.007, and b_1 equals 0.017, for unbleached and bleached kraft (both atmospheric and pressurized), respectively. As mentioned earlier, the intercept b_0 from the theoretical discussion is equal to 9/(8*Z*) (where *Z* is the zero-span strength) and should be used if available. If this is not available, as in this study, the intercept calculated from a regression analysis is subject to significant error. The coefficient b_1 is equal to γ in the modified Page equation 8. Nevertheless, the identity of b_1 for both pulps in this study indicates that this equation with b_1 = 0.017 and b_0 = 0.006 (the average of above) or determined from the measured value of *Z,* is applicable to all HCR pulps at least in our study.

Lastly, s/T and 1/T are substituted in the expression developed for TEA in equation 8:

$$TEA = \eta(0.5Ts) = \eta(0.5)\left(\frac{s}{T}\right)(T^2) = \eta(0.5)\frac{\left(\frac{s}{T}\right)}{\left(\frac{1}{T}\right)^2} \quad (8)$$

where η can be taken as approximately 1.3, which is found empirically from plots such as Fig. 11.

Thus, numerical values for TEA can be calculated using equations 13, 14, and 8 with the values of the equation coefficients a_0, a_1, b_0, b_1 and η given above for all HCR pulps in this study. For pulps different from those studied here, the procedure indicated above may have to be repeated to extract appropriate numerical values of the coefficients

in the equations. Generally, more experimental work is required to establish the repeatability and reproducibility of the coefficients.

The model described here is essentially composed of equations 13, 14, and 8. Equations 13 and 14 could be substituted in equation 8 to give TEA in terms of fibre curl, length, and pulp WRV directly and constitute the model expression of TEA. However, such an expression would be unwieldy.

In the next section, the model is applied to another data set of bleached kraft to validate the model as a predictor of TEA.

Validation of model

To verify the ability of the model to predict the *TEA* of a pulp, the model was applied using equations 11 and 12 to the data set of another HCR trial based on a more recent sample of bleached softwood kraft pulp (10 months more recent in sampling date). The correlation of the model prediction of 0.5 *T*.s (see equation 8) with the measured *TEA* is shown in Figure 14. Again, the measured *TEA* correlates well with 0.5*T*·s with a coefficient of 1.4, close to the value 1.3 in Fig. 11.

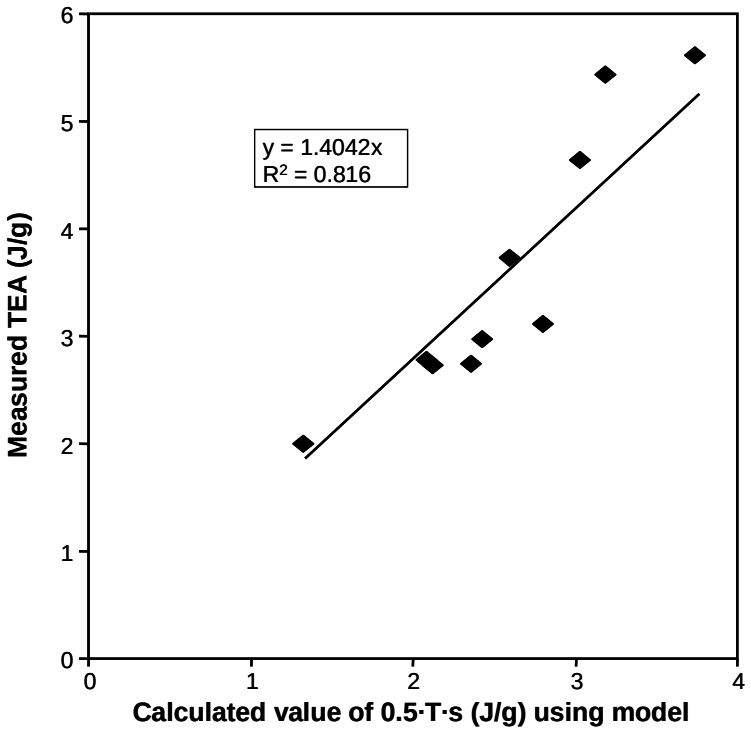

Fig. 14. To verify the ability of our model to predict the *TEA* of a pulp, the model was applied using equations 11 and 12 to the data set of another HCR trial based on a more recent sample of bleached kraft pulp.

This work indicates that the TEA of paper made from high-consistency refined pulp is primarily a function of the pulp properties of *WRV*, fibre curl, and fibre length. These properties are obviously affected by fibre morphology and refining parameters.

Discussion of the effect of fibre morphology on TEA is restricted to coarseness, because there is little in the literature on the subject. It is reported in the literature that increasing fibre coarseness increases stretch potential of fibres (Page and De Grâce 1976; Seth and Bennington 1995). Page and De Grâce conjectured that coarser fibres do not flex as readily under compressive stresses in the refining zone and suffer more local compression failure of the cell wall (Page and De Grâce 1976). However, increasing coarseness decreases the development of *WRV* (Abitz and Luner 1991) and hence decreases tensile strength significantly as predicted by the modified Page equation (see equation 7). Because TEA is a stronger function of tensile strength than normalized stretch (see equation 8), TEA decreases with increasing coarseness (see Fig. 15 for example). It is also noted that paper permeability increases with coarseness (Seth 1990) so that there is a compromise with respect to fibre coarseness for sack paper, which demands high *TEA* but low air resistance.

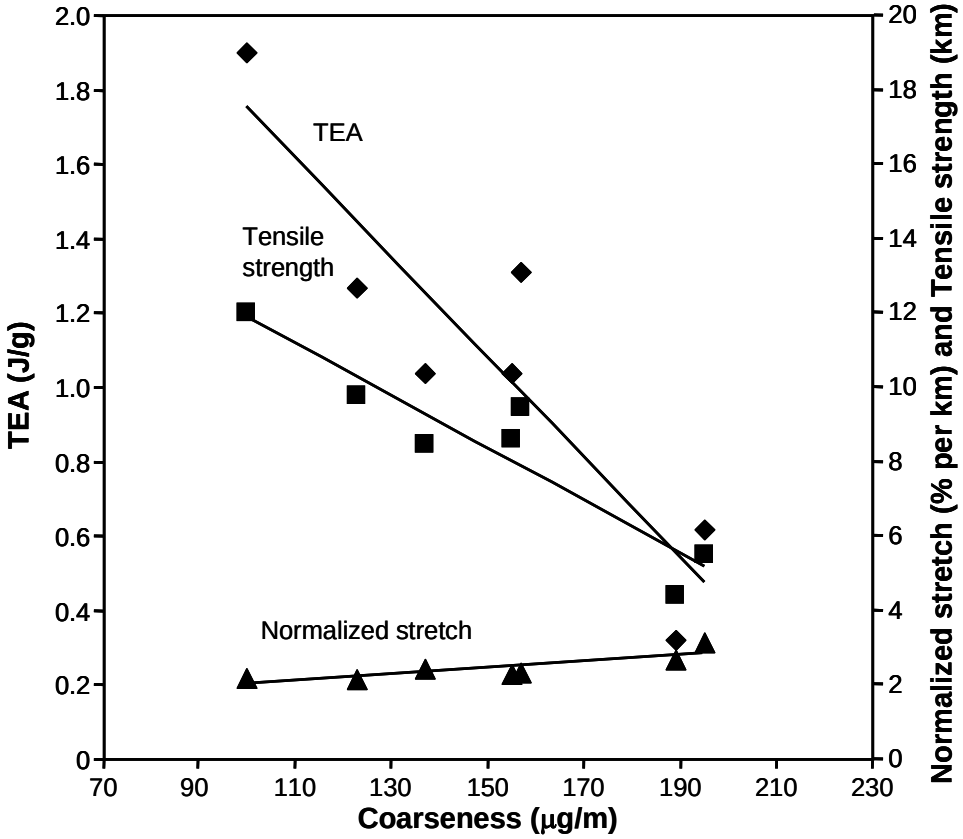

Fig. 15. The relationship between *TEA*, tensile, normalized stretch, and fibre coarseness is shown. Data were obtained from a study of pure wood species by Seth (1990).

Refining variables include specific energy, specific intensity, and refining pressure (atmospheric versus pressurized). Figure 16 indicates that at a given specific intensity (consistency, plate rotational speed and plate pattern), increasing refining energy with atmospheric pressure refining increases normalized stretch due to increased curl

induction and also increases tensile strength due to increased *WRV*, despite the curl increase. As a result, *TEA* increases significantly. However, with pressurized refining, increasing refining energy decreases normalized stretch due to decreasing curl but increases tensile strength due to increased *WRV*. As a result in this case, TEA only increases moderately with refining energy. Although pressurized refining gives less *TEA* development, air permeability is much less affected by refining energy, so that at the high air permeability demanded by sack paper the *TEA* of pressurized HCR is actually superior to atmospheric *HCR* (Gurnagul et al. 2009).

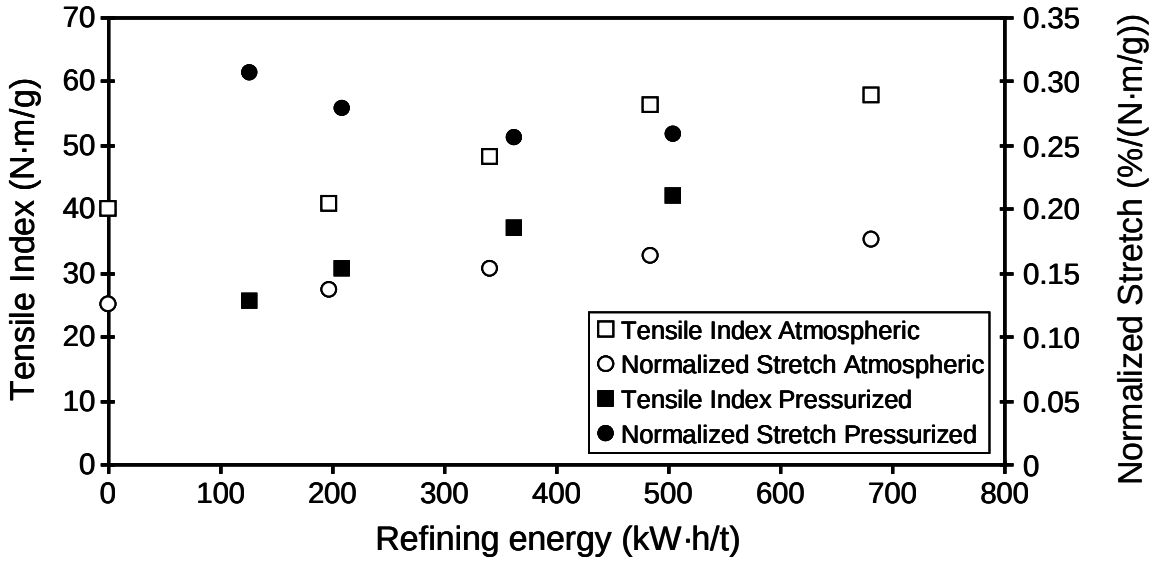

Fig.16. Effect of specific refining energy on normalized stretch and tensile index for atmospheric and pressurized HCR pulps.

CONCLUSION

A semi-empirical model has been developed to relate the tensile energy absorption (*TEA*) of high consistency refined (HCR) pulp to pulp properties including water retention value (*WRV*), fibre length, and fibre curl. *TEA* is shown to be related to the normalized stretch (ratio of stretch to tensile strength) and the tensile strength of the pulp. Normalized stretch appears to be a function of fibre curl, whereas tensile strength is a function of the fibre length, fibre curl, and *WRV* of the pulp. The manner in which these three pulp properties develop in a given refining operation determines the development of *TEA* for a given papermaking operation.

ACKNOWLEDGMENT

We would like to thank Dr. Reza Amiri for his comments on this manuscript.

REFERENCES CITED

Abitz, P., and Luner, P. (1991). "Relationship of wet fiber flexibility (WFF) to fiber and pulp properties," SUNY College of Environmental Science and Technology, *ESPRI Research Reports*, 94:V (Syracuse, NY), 125-126.

De Gennes, P.-G. (1979) "Scaling concepts in polymer physics," p. 40, Cornell University Press.

El-Hosseiny, F. (1994). "The effect of sheet densification on the shape of its stress-strain curve," *J. Pulp Paper Sci.* 20(12), J366-J370.

Gurnagul, N., Ju, S., and Shallhorn, P. (2006). "Optimizing high-consistency refining conditions for good sack paper quality," *Appita J*. 59 (6), 476-480.

Gurnagul, N., Shallhorn, P., Omholt, I., and Miles, K. (2009). "Pressurized high-consistency refining of kraft pulps for improved sack paper properties," *Appita J*. 62(1), 25-30.

Kibblewhite, R. P. (1976). "Fractures and dislocations in the walls of kraft and bisulphite pulp fibres," *Cellul. Chem. Technol.* 10(4), 497-503.

Mohlin, U.-B. (1975). Cellulose fibre bonding (3). "Effect of beating and drying on interfibre bonding," *Svensk Papperstid*. 78(9), 338-341.

Mohlin, U.-B., and Miller, J. (1992). "Influence of industrial beating on fibre swelling and fibre shape," SPCI-Aticelca 92, Eur. Pulp Paper week, Bologna Italy, 274-283.

Paavilainen, L. (1990). "Importance of particle size-fibre length and fines for the characterization of softwood kraft pulp," *Paperi ja Puu* 72(5), 516-526.

Paavilainen, L. (1993). "Conformability – flexibility and collapsibility of sulphate pulp fibres," *Paperi ja Puu* 75(9-10), 689-702.

Page, D. H. (1969). "A theory for the tensile strength of paper," *Tappi* 52(4), 674-681.

Page, D. H., and De Grâce, J. H. (1976). "The extensional behavior of commercial softwood bleached kraft pulps," *Tappi* 59(70), 98-101.

Page, D. H., Seth, R. S., Jordan, B. D., and Barbe, M. C. (1985). "Curl crimps, kinks and microcompressions in pulp fibres – Their origin, measurement and significance," *Papermaking Raw Materials, Trans. 8th Fund. Res. Symp.*, Vol. 1, 183-226, Oxford.

Patel, P. C., and Kothari, V. K. (2001). "Relationship between tensile properties of fibres and nonwoven fabrics," *Indian Journal of Fibre & Textile Research* 26(12), 398-402.

Seth, R. S. (1990). "Fibre quality factors in pulps II: The importance of fibre coarseness," Materials interactions relevant to pulp, paper and wood industries, *Mat. Res. Symp. Proc.* Vol. 197, 143-161.

Seth, R. S., and Bennington, C. P. J. (1995). "Fiber morphology and the response of pulps to medium-consistency fluidization," *Tappi* 78(12), 152-154.

Seth, R. S. (2001). "The zero span strength of papermaking fibres," *Pap. ja Puu* 83(8), 597-604.

Seth, R.S. (2005a). "Understanding sheet extensibility," *Pulp Paper Can.* 106(2), 33-40.

Seth, R.S. (2005b). "The importance of fibre straightness for pulp strength," Preprints, 91st annual meeting of PAPTAC, Book B, B37-B46.

Sjöberg, J. C., and Höglund, H. (2005). "Refining systems for sack paper pulp: Part I – HC refining under pressurized conditions and subsequent LC refining," *Nordic Pulp Pap. Res. J.* 20(3), 320-328.

APPENDIX

Derivation of L_{eff} in Equation 6

In Page's equation, L is the assumed uniform length of the straight fibres crossing the rupture line and pulled out at rupture. The mean pulled out length is $L/4$. It is tacitly assumed in the derivation of Page's equation that L refers to straight fibres *aligned in the direction of the applied tensile load*, which are perpendicular to the rupture line.

Assume a fibre slightly curled in a circular arc crossing the fracture line but globally aligned in the direction of the applied stress assumed perpendicular to the fracture line. Figure 1 illustrates this, but the curvature in the figure is exaggerated to show the geometry of the situation. For this curled fibre, those fibre segments, ds, aligned at an angle θ to the tensile load contribute to the observed tensile load a force equal to $\cos^3 \theta$ times the force of those fibre segments oriented at $\theta = 0$ (Van den Akker 1958). Because all of the fibres are assumed to be globally aligned in the direction of the applied load, the extra $\cos\theta$ factor found in reference 1 is not considered here. This is equivalent to an effective fibre length L_{eff} where $L_{eff} \le L$.

The angle of orientation θ constantly changes with position on the fibre curve. Here, $s = \theta R$ where s = the arc length along the fibre θ. At the fibre ends, $\theta = \pm L/2R$.

Therefore,

$$L_{eff} = \int_{-L/2}^{L/2} \cos^3(\theta) ds = \int_{-L/2}^{L/2} \cos^3(s/R) ds \quad \text{(A1)}$$

Integrating:

$$L_{eff} = [\frac{\sin(s/R)}{1/R} - \frac{\sin^3(s/R)}{3/R}]_{-L/2}^{L/2} = \frac{\sin(L/2R)}{1/R} - \frac{\sin(-L/2R)}{1/R} \quad \text{(A2)}$$

neglecting the terms including $\sin^3$(L/2R) for simplicity. Neglecting these terms increases the value of L_{eff} by about 20 % for C=0.1 and by 40 % for C=0.3.

Using a trigonometric identity for the difference of sines, we obtain:

$$L_{eff} = \frac{2\sin(L/2R)}{1/R} = \frac{L\sin(L/2R)}{L/2R} \quad \text{(A3)}$$

Now, for a circular arc, it can be shown easily that the curl index is given by

$$C = \frac{L/2R}{\sin(L/2R)} - 1. \quad \text{(A4)}$$

Finally, we arrive at

$$L_{eff} = \frac{L}{C+1} \quad . \tag{A5}$$

This was derived for a fibre curled slightly as a circular arc. It is assumed that this expression holds roughly true in Page's equation for fibres curled in more irregular ways.

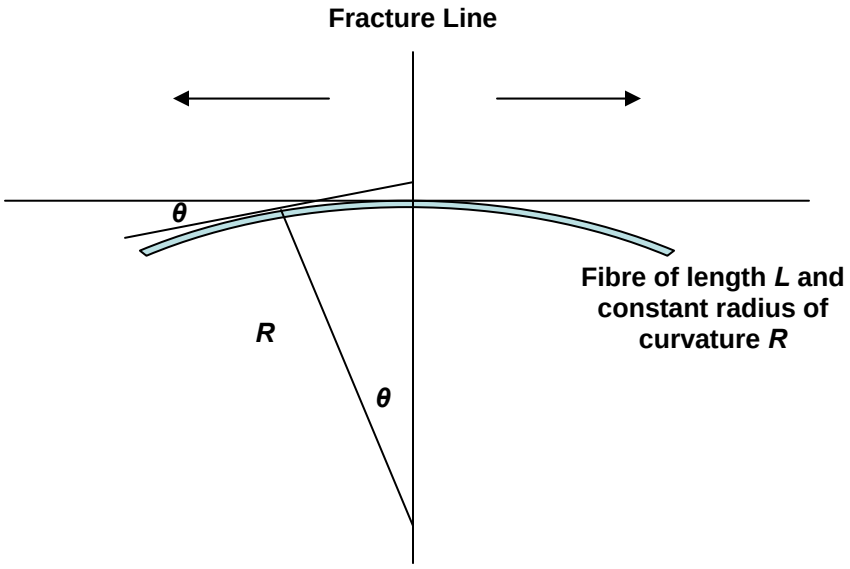

Fig. A1. Schematic drawing of curved fibre aligned in the direction of the applied stress

REFERENCES

Van den Akker, J. A., Lathrop, A. l., Voelker, M. H., and Dearth, L. R. (1958) "Importance of fiber strength to sheet strength," *Tappi* 41(8), 416-425.

Article submitted: January 13, 2009